NMR Temperature Measurements Using a Paramagnetic Lanthanide Complex

C. S. Zuo, K. R. Metz, Y. Sun, and A. D. Sherry*

*Department of Radiology, Beth Israel Deaconess Medical Center, Harvard Medical School, Boston, Massachusetts 02215; and *Department of Radiology, University of Texas Southwestern Medical Center, Dallas, Texas 75235-9085 and Department of Chemistry, University of Texas at Dallas, Richardson, Texas 75083-0688*

NMR thermometry has previously suffered from poor thermal resolution owing to the relatively weak dependence of chemical shift on temperature in diamagnetic molecules. In contrast, the shifts of nuclear spins near a paramagnetic center exhibit strong temperature dependencies. The chemical shifts of the thulium 1,4,7,10-tetraazacyclododecane-1,4,7,10-tetrakis(methylene phosphonate) complex (TmDOTP^{5-}) have been studied as a function of temperature, pH, and Ca^{2+} concentration over ranges which may be encountered *in vivo*. The results demonstrate that the ^{1}H and ^{31}P shifts in TmDOTP^{5-} are highly sensitive to temperature and may be used for NMR thermometry with excellent accuracy and resolution. A new technique is also described which permits simultaneous measurements of temperature and pH changes from the shifts of multiple TmDOTP^{5-} spectral lines. © 1998 Academic Press

Key Words: **paramagnetic thermometric substance; NMR temperature measurement; pH dependence; chemical shift; TmDOTP^{5-}.**

INTRODUCTION

The development of noninvasive, remote sensing methods for temperature measurements has attracted increasing attention in recent years. Interest in this technology has been motivated by traditional high-resolution NMR applications, as well as by the growing importance of medical hyperthermia and tissue ablation. Thus, a serious need has arisen for fast, sensitive, accurate, and preferably biocompatible NMR thermal mapping techniques (*1–12*). Most of the published methods involve chemical shift measurements using water or fluorocarbons as thermometric materials. The major obstacles to the use of these substances are the weak temperature dependencies of the water ^{1}H and fluorocarbon ^{19}F shifts (*3, 4, 7, 11, 13, 14*), especially for *in vivo* applications requiring high thermal resolution (e.g., ≤1°C) at clinical magnetic field strengths (≤1.5 T). Even conventional studies performed with high-resolution spectrometers would benefit from the availability of compounds with greater temperature sensitivities.

It is well known that the chemical shifts of nuclear spins in paramagnetic complexes are strongly dependent on temperature (*15–20*). This phenomenon has recently been exploited for

in vivo NMR thermometry (*21–23*), and a preliminary investigation of the thermometric properties of thulium 1,4,7, 10-tetraazacyclododecane-1,4,7,10-tetrakis(methylene phosphonate) (TmDOTP^{5-}) has been published (*21*). Since this lanthanide complex appears to have relatively low toxicity, it is potentially attractive for *in vivo* applications (*24–26*). The present work was undertaken to explore more thoroughly the properties and use of TmDOTP^{5-} for NMR thermometry. The chemical shifts of ^{1}H and ^{31}P in the complex have been characterized as a function of temperature, pH, and other factors which may be encountered during NMR temperature measurements *in vivo*. A method is also presented which allows both temperature and pH to be monitored simultaneously by using the chemical shifts of two nuclei in the complex.

THEORETICAL CONSIDERATIONS

In a paramagnetic lanthanide complex, the total chemical shift of a nuclear spin (δ_t) is the sum of diamagnetic (δ_d) and paramagnetic components (δ_e):

$$\delta_t = \delta_d + \delta_e. \quad [1]$$

The diamagnetic term can have both intramolecular and intermolecular contributions from ring currents, chemical exchange, and protonations. For a nuclear spin in the vicinity of an unpaired electron, it has been established that Fermi contact interactions contribute paramagnetic shielding terms in T^{-1} and that pseudocontact interactions provide terms in both T^{-1} and T^{-2} (*15, 17, 18, 20*). It is important to note that δ_e is typically much larger than δ_d, and that δ_e depends strongly on temperature while δ_d has very weak or no temperature dependence (*20*). Consequently, the effect of temperature on NMR chemical shifts in paramagnetic complexes is nearly always dominated by δ_e.

The paramagnetic chemical shift component δ_e also depends on the vector **r** between the nuclear spin and the

unpaired electron (*17, 18, 20*), so factors affecting **r** will influence the experimental shift. One such factor is pH, since protonation of the complex can alter the molecular geometry and change the relative contact/pseudocontact shift. The variation of the total chemical shift δ_t under conditions where both temperature and pH change simultaneously can be described as

$$\Delta\delta_t = C_T \cdot \Delta T + C_{\text{pH}} \cdot \Delta\text{pH}, \qquad [2]$$

where $C_T = (\partial\delta_t/\partial T)_{\text{pH}}$ is the temperature dependence of chemical shift, and $C_{\text{pH}} = (\partial\delta_t/\partial\text{pH})_T$ is the pH dependence of chemical shift. Equation [2] may not, in general, be used to obtain temperature and pH changes directly from chemical shift because C_T and C_{pH} may be functions of both temperature and pH. For example, C_T can vary at different pH values if the molecular geometry changes, and C_{pH} may be a function of temperature due to the **r**-dependence and temperature dependence of δ_e. pH and temperature contributions are, therefore, not separable from each other. For Eq. [2] to be applicable for practical temperature measurements, it is necessary that molecular geometry remain unaffected by pH changes (i.e., $(\partial\mathbf{r}/\partial\text{pH})_T = 0$). In that case C_T is independent of pH, C_{pH} is approximately independent of temperature, and contributions from temperature and pH are separable. It will be shown that this is a very good approximation from 25 to 45°C for the complex TmDOTP^{5-} within the pH range of 6 to 8. Equation [2] thus becomes a simple bivariable linear equation, enabling ΔT and ΔpH to be calculated simultaneously from the chemical shifts of two nonequivalent spins provided values of C_T and C_{pH} have already been established.

The chemical shifts of ^{31}P and ^{1}H in TmDOTP^{5-} may also be functions of the concentration of diamagnetic binding ions such as Ca^{2+} (*27*). Using an argument analogous to that outlined earlier for pH, it is clear that Ca^{2+} binding does not alter the total chemical shift temperature dependence provided the molecular geometry remains unchanged. Instead, the effects will manifest through the diamagnetic term and, like pH, they will be small compared to those of temperature. Ca^{2+} binding and similar phenomena can be represented by adding appropriate terms to Eq. [2]. Similarly, simultaneous changes in temperature, pH, and Ca^{2+} concentration can be determined from the chemical shifts of three nonequivalent spins.

In summary, for a lanthanide complex to be most useful as an NMR thermometric substance it is important that the temperature dependence of the chemical shift (C_T in Eq. [2]) for the spin in question be independent of other factors which may vary simultaneously with temperature. This criterion is satisfied provided the electron–nuclear distance and angles are independent of pH, Ca^{2+} concentration, and so forth.

EXPERIMENTAL METHODS

All studies were performed with aqueous solutions containing 20 mM TmDOTP^{5-} (sodium salt, Magnetic Resonance Solutions, Dallas, TX). A Beckman model 40 pH meter was used to measure solution pH values, which were adjusted in the range of 4 to 10 by adding 0.1 M NaOH or H$_2$SO$_4$. For solutions in D$_2$O, pD was adjusted with NaOD or D$_2$SO$_4$, and pD values were obtained by adding 0.40 to the pH reading (*28*). To investigate the effect of Ca^{2+} binding, 20 mM TmDOTP^{5-} solutions containing 2.6 and 5.3 mM CaCl$_2$ were also studied. Chemical shifts of ^{1}H and ^{31}P in TmDOTP^{5-} were measured using a 7.06-T General Electric GN-300WB spectrometer with a 10-mm probe. Fully relaxed data were acquired using a simple one-pulse sequence with 90° pulses (26 μs for ^{1}H; 19 μs for ^{31}P), a cycle time of 26 ms, and 20–100 averages, yielding a total data collection time of ≤2.6 s. This gave a signal/noise (*S/N*) of 40:1 to 230:1 for the various peaks in TmDOTP^{5-}. It was found that proton signals from the complex could be detected in H$_2$O solutions by using solvent suppression and narrow-band excitation techniques. However, studies of solutions in deuterium oxide (99.9%, Cambridge Isotopes, Woburn, MA) proved more convenient, and all results reported here were obtained using this solvent. Proton chemical shifts were measured relative to either internal sodium 3-(trimethylsilyl)propionate-2,2,3,3-d_4 (TSP) at 0 ppm or the HOD signal at 4.7 ppm, since water is a convenient reference for *in vivo* work. The slight temperature dependence of the water resonance frequency was negligible compared to that of the complex, and any effect on the reported shifts is within the experimental uncertainty. ^{31}P chemical shifts were referenced to external 85% phosphoric acid contained in a spherical microcell. Shifts to high frequencies (i.e., "downfield") were designated as positive. Sample temperatures were regulated in the range of 25 to 45°C using the standard GE variable temperature controller. The accuracy of the temperature controller was verified independently by using a 10-mm sample tube of water containing either a thermometer or a YSI #44031 thermistor (Yellow Springs Instrument Co., Yellow Springs, OH). Sample temperatures were found to be within 1°C of the set value. Spin–lattice relaxation times were obtained by the inversion recovery technique using 19 delay values. TmDOTP^{5-} linewidths were measured from shimmed samples so that contributions of static field inhomogeneities were less than 2% in the worst case.

RESULTS

The experimental measurements focused on ^{31}P and ^{1}H, as these have greater NMR sensitivities than the other nuclides in TmDOTP^{5-}. The complex contains six magnetically nonequivalent groups of protons, previously designated as H$_1$ to H$_6$ (*29*), and four magnetically equivalent phosphorus atoms due to its fourfold symmetry (Fig. 1). Chemical shifts were
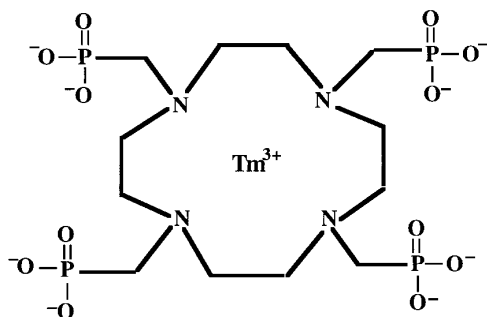
FIG. 1. Molecular structure of TmDOTP^{5-}. The complex contains six magnetically nonequivalent groups of protons, but all four phosphorus atoms are equivalent because of the fourfold symmetry.

measured for all six proton signals and for phosphorus. The H$_1$, H$_5$, and H$_6$ peaks were shifted downfield while the H$_2$, H$_3$, and H$_4$ lines were shifted upfield, as reported previously (29). Shifts of the TmDOTP^{5-} protons varied linearly with temperature over the 25 to 45°C range, with each type of proton exhibiting a unique temperature dependence C_T and linewidth (Table 1). H$_1$ and H$_3$, for example, had chemical shift temperature dependencies of $+1.08$ and -0.42 ppm/°C, respectively (Fig. 2a), and linewidths of 1.89 and 0.86 ppm at 25°C. The temperature dependence of the H$_6$ shift was 0.87 ppm/°C (Fig. 2b), and this line had a width of 0.63 ppm. The ^{31}P resonance line had a width of 1.05 ppm and was shifted 350.7 ppm upfield from 85% phosphoric acid at 25°C (29). As with the protons, the ^{31}P chemical shift was linearly dependent on temperature (Fig. 2b) and had a slope of 2.18 ± 0.02 ppm/°C ($r^2 = 0.999$) over the temperature range of 25 to 45°C (21).

Both ^{1}H and ^{31}P relaxed rapidly (Table 1) because of the unpaired metal electrons. Inversion recovery measurements at

25°C gave T_1 values of 0.53, 1.8, and 2.4 ms for H$_1$, H$_6$, and ^{31}P, respectively. Relaxation was less efficient when the temperature was increased to 37°C. This temperature dependence and the short T_1 values both suggest dipolar relaxation dominated by interactions between the unpaired electron and the nuclear spins (20). Measured values for T_1 and T_2 were the same within experimental uncertainty, also consistent with this mechanism operating in the extreme narrowing regime.

To achieve optimum temperature resolution from chemical shift measurements on a single signal, an intense line should be chosen which has both a narrow width and a shift which is strongly temperature dependent. Since all six ^{1}H lines in Tm-DOTP^{5-} have equal areas, using a narrow line not only improves NMR sensitivity but also makes it easier to detect chemical shift differences due to temperature changes. Thus, the absolute value of the C_T/full width at half maximum (FWHM) ratio may be used as a rational criterion for selecting the best line (bottom row of Table 1). Among the proton signals, H$_6$ had the most favorable combination of chemical shift temperature dependence and linewidth, and all discussions of ^{1}H in the remainder of this paper refer to H$_6$ unless otherwise noted.

Depending on their locations within the molecule, the chemical shifts of protons in TmDOTP^{5-} may be influenced by the electric fields from the negatively charged phosphonate groups (29). One oxygen atom in each of the four magnetically equivalent phosphonate ($-PO_3^{2-}$) groups is coordinated to Tm^{3+} while another is capable of protonation or binding a cation (Fig. 1). The four pK_a's corresponding to these protonations have been published (30) and are 8.25, 6.88, 5.64, and 4.47. These values were determined by potentiometry in 0.1 M tetramethylammonium chloride and may differ when other

TABLE 1
Summary of Chemical Shifts, Temperature Dependencies, Linewidths, and Relaxation Times
for ^{1}H and ^{31}P in TmDOTP^{5-} from 25 to 45°C

	H$_1$	H$_2$	H$_3$	H$_4$	H$_5$	H$_6$	^{31}P
Shift (ppm) at 25°C[a]	−193.7	+92.8	+72.7	+513.6	−398.9	−155.7	−350.7
C_T (ppm/°C)[b]	1.08	−0.54	−0.42	−2.88	2.19	0.87	2.18
	±0.09	±0.05	±0.04	±0.19	±0.11	±0.03	±0.02
FWHM (ppm) at 25°C[c]	1.89	0.99	0.86	3.77	2.23	0.63	1.05
FWHM (ppm) at 37°C[c]	1.67	—	—	—	—	0.60	0.94
T_2 (ms) at 25°C[d]	0.56	1.1	1.2	0.28	0.48	1.7	2.5
T_2 (ms) at 37°C[d]	0.63	—	—	—	—	1.8	2.8
T_1 (ms) at 25°C[e]	0.53	—	—	—	—	1.8	2.4
T_1 (ms) at 37°C[e]	0.56	—	—	—	—	2.0	3.1
$|C_T$/FWHM$|$[f]	0.57	0.55	0.48	0.76	0.98	1.45	2.08

[a] Chemical shift with respect to TSP or 85% phosphoric acid. pH = 7.6; [Ca^{2+}] = 0 mM.
[b] Slope of a linear least-squares fit to chemical shift versus temperature data from 25 to 45°C.
[c] Full linewidth at half-maximum height. Estimated uncertainty = ±5%.
[d] Spin–spin relaxation time calculated from $T_2 = (\pi \cdot \text{FWHM})^{-1}$, with FWHM in hertz. Estimated uncertainty = ±5%.
[e] Spin–lattice relaxation time measured by inversion recovery. Estimated uncertainty = ±10%.
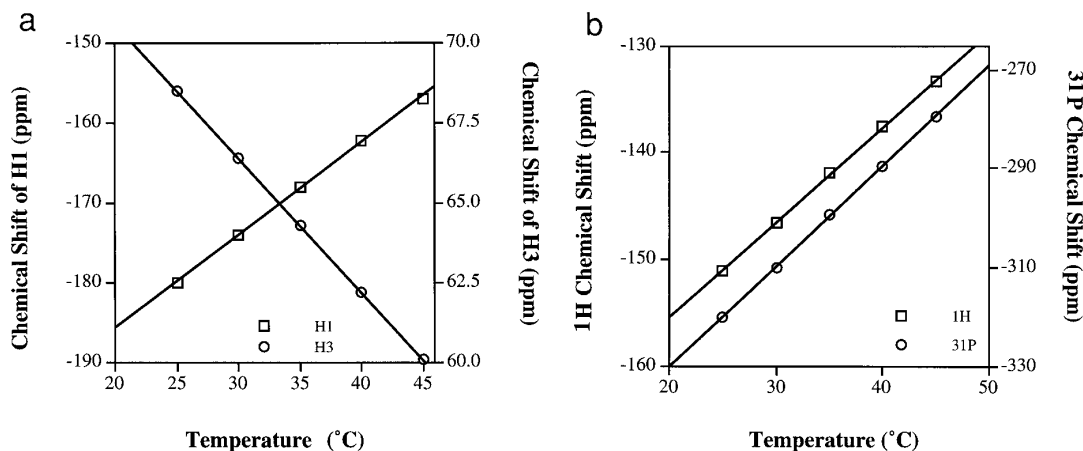[f] Absolute value of the ratio of shift temperature dependence (in ppm/°C) and line width at 25°C (in ppm).

FIG. 2. (a) Plot of chemical shift versus temperature for TmDOTP^{5-} protons H$_1$ (squares) and H$_3$ (circles). Least-squares line fitting gave C_T = +1.08 ppm/°C for H$_1$ (r^2 = 0.999) and C_T = −0.42 ppm/°C for H$_3$ (r^2 = 1.000). (b) Plot of chemical shift versus temperature for TmDOTP^{5-} proton H$_6$ (squares) and ^{31}P (circles). Least-squares line fitting gave C_T = +0.87 ppm/°C for H$_6$ (r^2 = 0.995) and C_T = +2.18 ppm/°C for ^{31}P (r^2 = 0.999).

salts such as NaCl are present. ^{31}P shifts are also sensitive to small variations in local charge density and conformation that accompany pH changes. Measurements of chemical shift versus pH for the H$_6$ proton line and the ^{31}P signal in TmDOTP^{5-} yielded typical titration curves (*21*). The linear portion of the ^{31}P curve (Fig. 3) had a slope C_{pH} of −15.32 ppm/pH unit. The chemical shift of ^{1}H in TmDOTP^{5-} was found to vary by approximately 8.5 ppm between pH 4.5 and 11. The circles in Fig. 3 show the linear portion of the ^{1}H shift versus pH curve, with a slope C_{pH} of −3.27 ppm/pH unit. Values of C_T for ^{1}H and ^{31}P have been shown (*21*) to be independent of pH within the linear region of the shift versus pH curve from approximately pH 6 to 8.

The shifts of ^{1}H and ^{31}P were previously found to be independent of the TmDOTP^{5-} concentration in the range of ≤40 mM (*21*), as expected for a stable complex. However, the binding of various cations to TmDOTP^{5-} can also cause chemical shifts to occur. Ca^{2+} is known to compete with Na$^+$ for binding sites on TmDOTP^{5-} (*27*), so measurements were performed using TmDOTP^{5-} solutions containing Ca^{2+} to determine if Ca^{2+}–Na$^+$ exchange affected the temperature dependence of the chemical shifts. As with the pH effect, the slope of the shift versus temperature data for ^{1}H and ^{31}P in TmDOTP^{5-} was found to remain constant at Ca^{2+} concentrations of up to 5.3 mM, while the intercept varied slightly (Fig. 4). Thus, the temperature dependence of the chemical shift C_T was invariant over this Ca^{2+} concentration range, but the absolute value of the shift was weakly dependent on Ca^{2+} level.

Chemical shifts were measured for proton H$_6$ and ^{31}P of TmDOTP^{5-} in a process where temperature and pH were allowed to change simultaneously. The results for five different combinations of temperature and pH settings are summarized in Table 2. Changes in temperature and pH (ΔT_{NMR} and

ΔpH_{NMR}) were then calculated using the solution of Eq. [2] for two independent chemical shifts

$$\Delta T_{NMR} = \frac{\Delta \delta_t^H \cdot C_{pH}^P - \Delta \delta_t^P \cdot C_{pH}^H}{C_T^H \cdot C_{pH}^P - C_T^P \cdot C_{pH}^H} \quad \text{and} \quad [3]$$

$$\Delta pH_{NMR} = \frac{\Delta \delta_t^P \cdot C_T^H - \Delta \delta_t^H \cdot C_T^P}{C_T^H \cdot C_{pH}^P - C_T^P \cdot C_{pH}^H}, \quad [4]$$

where superscripts H and P represent ^{1}H and ^{31}P, respectively. The following values were used for the four constants in Eqs. [3] and [4]: C_T^H = +0.87 ppm/°C, C_T^P = +2.18 ppm/°C, C_{pH}^H = −3.27 ppm/pH unit, and C_{pH}^P = −15.32 ppm/pH unit. Temperature and pH changes measured by NMR, which are tabulated in the last two columns of Table 2, typically agreed with
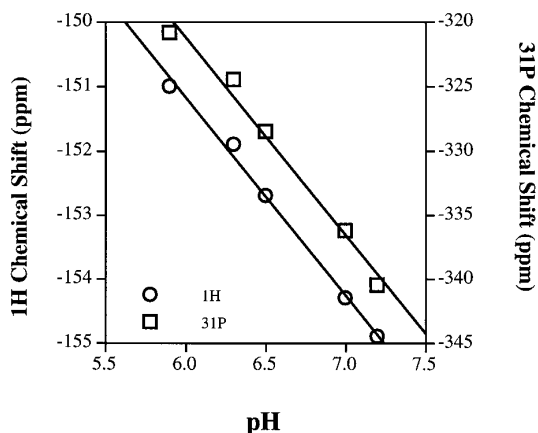

FIG. 3. Plot of chemical shift versus pH for TmDOTP^{5-} proton H$_6$ (circles) and ^{31}P (squares) at 25°C. Least-squares line fitting gave C_{pH} = −3.27 ppm/pH unit for H$_6$ (r^2 = 0.994) and C_{pH} = −15.32 ppm/pH unit for ^{31}P (r^2 = 0.985).
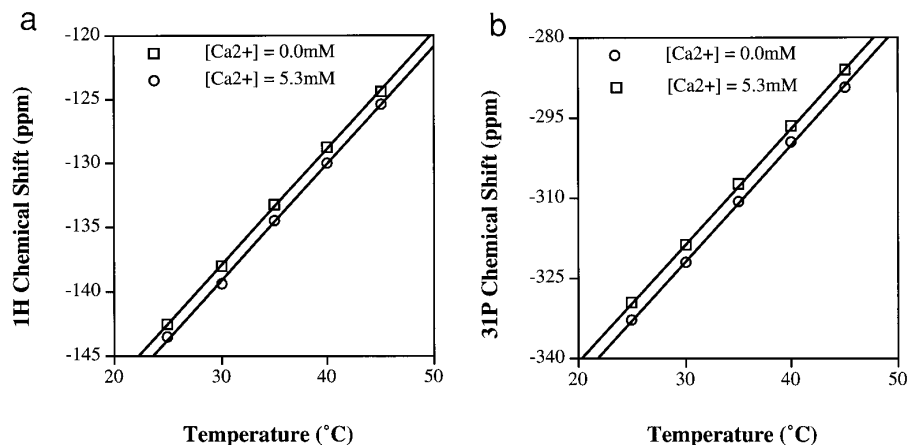
FIG. 4. (a) Chemical shifts versus temperature for proton H_6 in 20 mM aqueous $TmDOTP^{5-}$ at various Ca^{2+} concentrations. Best-fit slopes C_T were found to be 0.87 ppm/°C for 0.0 mM Ca^{2+} ($r^2 = 0.995$), 0.91 ppm/°C for 2.6 mM Ca^{2+} ($r^2 = 0.999$), and 0.89 ppm/°C for 5.3 mM Ca^{2+} ($r^2 = 1.00$). The data for 2.6 mM Ca^{2+}, which lie between those of the 0 mM and 5.3 mM solutions, have been omitted for clarity. (b) Chemical shifts versus temperature of ^{31}P in 20 mM aqueous $TmDOTP^{5-}$ at various Ca^{2+} concentrations. Best-fit slopes C_T were found to be 2.18 ppm/°C for 0.0 mM Ca^{2+} ($r^2 = 0.999$), 2.16 ppm/°C for 2.6 mM Ca^{2+} ($r^2 = 0.999$), and 2.17 ppm/°C for 5.3 mM Ca^{2+} ($r^2 = 1.00$). The data for 2.6 mM Ca^{2+} have been omitted for clarity.

set values to within a few tenths of a degree and 0.1 pH unit. For example, between experiments 1 and 4 the sample temperature setting was increased by 10.0°C while the pH was decreased by 0.9 units. This resulted in proton and ^{31}P chemical shift changes of +12.1 and +37.5 ppm, respectively. Using these shifts in combination with Eqs. [3] and [4] gave measured changes of +10.1°C and −1.0 pH unit, in good agreement with the set values.

DISCUSSION

The NMR spectral characteristics of a specific nucleus in $TmDOTP^{5-}$ would be expected to correlate with the position of that nucleus relative to the unpaired electron at the center of the complex. Pseudocontact interactions between the electron and neighboring nuclei cause the sign and magnitude of the local field to vary with both the electron–nuclear distance and the angles. Strong pseudocontact interactions result when the electronic g-factor is anisotropic or if the ligand field symmetry is less than cubic, and these effects on local field at the nucleus are not averaged by molecular tumbling (17). The local field itself can produce large chemical shifts while temporal modulations of this field result in efficient relaxation and broad lines. Furthermore, since both the chemical shift and its temperature dependence are dominated by components of the paramagnetic shielding term, values of C_T should be correlated with the shift. This is indeed the case, as demonstrated convincingly by a plot of C_T versus shift (Fig. 5) formed by using data for the six types of protons from Table 1. The plot intercept is very near 0 ppm/°C, which is consistent with the very small shift temperature dependence known to be exhibited by diamagnetic compounds such as water. Since a large chemical shift temperature dependence is one desirable property for a thermo-

metric substance, Fig. 5 implies that compounds with the greatest absolute chemical shifts are likely to be the most promising candidates for use in NMR thermometry. This supports recent conclusions based on plots of data from nuclides in several different lanthanide complexes (21). Figure 5 allows calculation of the chemical shift range over which proton C_T values can be assumed to remain constant. For example, if a C_T variation of ±0.10 ppm/°C is acceptable, then the chemical shift may vary by approximately ±18 ppm. This corresponds to a temperature change of about ±20°C for proton H_6. High-accuracy temperature measurements outside this range would probably require the use of a slightly adjusted value for C_T. Alternatively, the expression $C_T^H = -0.00557\delta_t^H - 0.0143$ could be substituted into Eqs. [2], [3], and [4].

Although $TmDOTP^{5-}$ protons with large absolute chemical shifts also tend to have large linewidths (Table 1), the correlation is not as strong as that for C_T in Fig. 5. This is presumably because the nuclear spin–spin relaxation rate depends on a combination of the correlation times associated with electronic relaxation, molecular tumbling, and segmental motions within the complex. Consequently, even two nuclei which fortuitously experience the same average local field may not have identical overall correlation times or, therefore, linewidths. This also explains why the parameter $|C_T/FWHM|$ in Table 1 is not simply a constant, making some signals more useful for thermometry than others.

Because the chemical shifts of $TmDOTP^{5-}$ depend so strongly on temperature, outstanding thermal resolution can be achieved using this complex. Resolution can be defined as the smallest temperature difference that may be relied upon to produce a detectable chemical shift change. Simulations were performed for the H_6 peak, the narrowest proton signal in the spectrum, to examine the practical effect of spectral S/N on

TABLE 2
Comparison of Set and Measured Temperature and pH Values in a Process
Where Both Temperature and pH Changed Simultaneously

Experiment	T_{set}	pH_{set}	δ_t^H	δ_t^P	Comparison	$\Delta\delta_t^H$	$\Delta\delta_t$	Set values		Values measured by NMR	
								ΔT_{set}	ΔpH_{set}	ΔT_{NMR}	ΔpH_{NMR}
1	25.0	7.2	−154.9	−340.5	—	—	—	—	—	—	—
2	30.0	6.5	−147.9	−317.5	2 vs 1	+7.0	+23.0	+5.0	−0.7	+5.2	−0.8
3	30.0	7.0	−149.6	−325.7	3 vs 1	+5.3	+14.8	+5.0	−0.2	+5.3	−0.2
					3 vs 2	−1.7	−8.2	0.0	+0.5	+0.1	+0.6
4	35.0	6.3	−142.8	−303.0	4 vs 1	+12.1	+37.5	+10.0	−0.9	+10.1	−1.0
					4 vs 2	+5.1	+14.5	+5.0	−0.2	+5.0	−0.2
					4 vs 3	+6.8	+22.7	+5.0	−0.7	+4.8	−0.8
5	40.0	6.3	−138.2	−291.9	5 vs 1	+16.7	+48.6	+15.0	−0.9	+15.6	−0.9
					5 vs 2	+9.7	+25.6	+10.0	−0.2	+10.5	−0.2
					5 vs 3	+11.4	+33.8	+10.0	−0.7	+10.3	−0.7
					5 vs 4	+4.6	+11.1	+5.0	0.0	+5.5	+0.1

Note. All temperatures (T) and temperature changes (ΔT) are in °C. Chemical shifts (δ_t) and chemical shift changes ($\Delta\delta_t$) are in ppm. Superscripts H and P represent ^{1}H and ^{31}P, respectively. Measured temperature and pH changes were calculated with Eqs. [3] and [4] from the chemical shifts of H_6 and ^{31}P using the constants $C_T^H = +0.87$ ppm/°C, $C_T^P = +2.18$ ppm/°C, $C_{pH}^H = -3.27$ ppm/pH unit, and $C_{pH}^P = -15.32$ ppm/pH unit.

thermal resolution. For a 20 mM solution of the complex, 100 averages produced $S/N = 230$ for this peak in only 2.6 s, and the corresponding resolution was found to be 0.01 to 0.02°C. For $S/N = 10$, the resolution degraded to approximately 0.1°C. Thus, under the conditions of these experiments, 0.1°C thermal resolution is possible in 2–3 s using a TmDOTP^{5-} concentration of 1 mM. It is important to recognize that this level of performance can only be achieved under optimum conditions typical of traditional high-resolution studies (i.e., when the temperature is temporally stable and spatially uniform, and static field inhomogeneities are much smaller than the natural linewidth). Serious deviations from these conditions will result in the loss of performance. For example, a recent *in vivo* study at 4.7 T (*21*) found substantial broadening of the H$_6$ line (FWHM = 2.7 ppm) so that a 0.5-min acquisition was required to produce $S/N = 65$ and a thermal resolution of approximately 0.5°C.

A promising alternative method for measuring temperature is to combine the chemical shifts of two nonequivalent Tm-DOTP^{5-} spins, one shifted upfield and the other shifted downfield, to provide a larger shift temperature dependence than that obtainable from one shift alone. For instance, the combination H$_6$–H$_3$ provides an effective temperature dependence of 1.3 ppm/°C, much higher than the combination of H$_6$–H$_1$ where both signals are shifted in the same direction (Fig. 6), about one order of magnitude larger than the H$_{ax\ 1}$ and H$_{ac}$ combination in YbDOTMA (*23*), and more than two orders of magnitude greater than ^{1}H in water (Fig. 6) and ^{19}F in perfluorocarbons (*4, 11*). Another advantage of using a shift difference between two TmDOTP^{5-} lines is that spatial or temporal variations in bulk susceptibility do not necessarily compromise the temperature measurement. If the temperature change itself does not

cause a large variation (i.e., >0.5 ppm) in bulk susceptibility compared to the linewidth, accurate relative thermal measurements are still possible. Even if susceptibility differences occur, it should still be possible to measure the chemical shifts of two TmDOTP^{5-} signals in the same spatial volume, using the difference to obtain the temperature without bulk susceptibility errors.

In a biological application such as hyperthermia, it is common for simultaneous changes in pH and temperature to occur in the heated region. The pH value is often a sensitive indicator
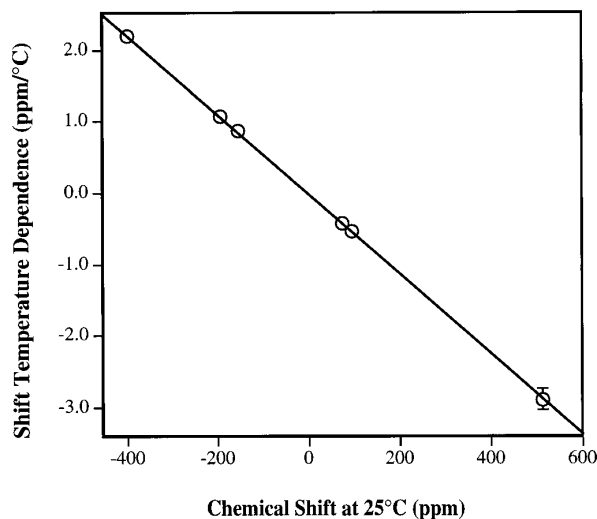

FIG. 5. Plot of chemical shift temperature dependence (C_T) versus chemical shift (δ_t) at 25°C for the six types of protons in TmDOTP^{5-}. Shifts are relative to that of TSP at 0 ppm. Best-fit slope and intercept were −0.00557 °C^{-1} and −0.0143 ppm/°C, respectively ($r^2 > 0.9999$).
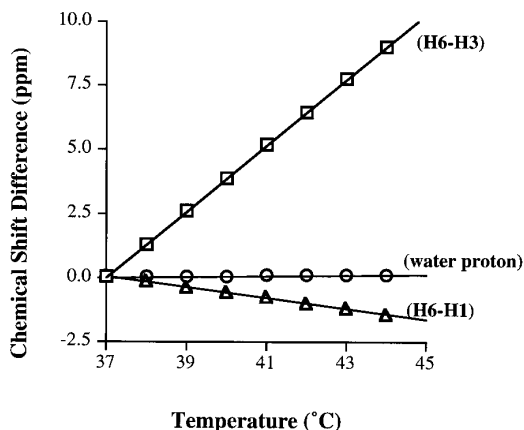
FIG. 6. Temperature-dependent changes in the chemical shift difference between protons in TmDOTP^{5-}. So that all curves could be depicted on the same scale, values were arbitrarily adjusted to zero at 37°C and only the changes were plotted as a function of temperature. While increasing temperature decreased the chemical shift difference between H$_6$ and H$_1$, the H$_6$–H$_3$ shift difference increased dramatically. Changes in the water proton shift are included for comparison. Linear least-squares fits gave slopes of 1.28 ppm/°C for H$_6$–H$_3$ ($r^2 = 1.00$), −0.21 ppm/°C for H$_6$–H$_1$ ($r^2 = 1.00$), and 0.01 ppm/°C for HOD ($r^2 = 1.00$).

of the physiological status of the tissue; hence, it may be important to measure the pH as the treatment is proceeding. The ^{31}P and ^{1}H chemical shifts in TmDOTP^{5-} were found to be linearly dependent on pH over the pH 6–8 range relevant to hyperthermia (Fig. 3). However, the temperature dependencies of the ^{31}P and ^{1}H shifts exhibited little sensitivity to pH (<5%) in this pH range. Thus, within the linear portion of the δ versus pH titration curve, the protonation of PO$_3^{2-}$ groups did not significantly alter the geometry of the complex, and the chemical shift pH dependence was dominated by diamagnetic electric field effects alone. Consequently, the pH effect and temperature contribution could be separated by the method detailed in the theoretical discussion (Eq. [2]), enabling the chemical shifts of ^{31}P and ^{1}H in TmDOTP^{5-} to be used to measure temperature and pH simultaneously (Table 2). The advantages of using TmDOTP^{5-} for measuring pH *in vivo* are that it is relatively noninvasive, offers adequate pH resolution, and does not require extra hardware. However, it should be noted that TmDOTP^{5-} would measure extracellular pH because it does not enter cells (27). Although ^{31}P and H$_6$ signals were used here for simultaneous pH and temperature measurements, similar results could be obtained by using a pair of proton lines. Also, a related multiparametric treatment should allow absolute, as opposed to relative, temperature measurements to be performed.

The chemical shift temperature dependencies of ^{31}P and ^{1}H in TmDOTP^{5-} remained unchanged as the concentration of Ca^{2+} was varied (Fig. 4), similar to the effects observed for pH. The absolute values of the chemical shifts changed weakly as the Ca^{2+} concentration increased from 0 to 5.2 mM, implying that exchange of Ca^{2+} for Na$^+$ imposed a small perturba-

tion on the local field. This suggests that the influence of Na$^+$/Ca^{2+} exchange on the chemical shifts was through the diamagnetic term. As discussed earlier, one can conclude that the electron–nuclear distances and angles were unaffected by the exchange process or, more generally, that the geometry of the complex was independent of Ca^{2+} concentration. The cation binding issue may complicate the use of TmDOTP^{5-} in cases where substantial Ca^{2+} concentration changes accompany other processes of interest (i.e., temperature changes). However, even for relatively large variations it should still be possible to measure simultaneous changes in temperature, pH, and Ca^{2+} concentration from the shifts of several independent peaks in a system of linear equations. The rapid relaxation of ^{31}P and ^{1}H in TmDOTP^{5-} should permit these shifts to be determined in a matter of seconds for many applications.

While the chemical, biological, and NMR properties of TmDOTP^{5-} make it attractive both for *in vivo* and for more traditional NMR thermometry investigations, it should be noted that this complex is just one member of a large family of lanthanide complexes. It is possible that other metal and ligand combinations may prove superior to the one described here. For example, lower sensitivity of the chemical shifts to the binding of metal cations such as Ca^{2+} would be an asset in many applications, although greater sensitivity would be desirable if measurements of such cations were the objective. Additional studies might also reveal specific lanthanide complexes having even lower toxicity, greater or smaller pH dependence, and perhaps even better temperature sensitivity. The excellent performance of TmDOTP^{5-} in the present study demonstrates the value of using lanthanide complexes for NMR thermometry, making a survey of other metal/ligand combinations worthwhile.

SUMMARY

The large temperature dependencies of the chemical shifts of nuclear spins in paramagnetic lanthanide complexes may be used for NMR temperature measurements. Using the chemical shifts of ^{1}H and ^{31}P in TmDOTP^{5-} as an example, we have investigated the properties of lanthanide complexes for NMR thermometry under conditions relevant to both high-resolution and *in vivo* applications. Experimental studies demonstrate that, compared to the diamagnetic NMR thermometric materials currently employed, TmDOTP^{5-} enables much more sensitive temperature measurements to be performed. Simultaneous changes in temperature and pH can also be determined quickly and accurately from the shifts of multiple independent peaks in the spectrum of this complex. Rapid spin–lattice relaxation in TmDOTP^{5-} permits massive signal averaging in a very short time so that high S/N may be achieved even with low concentrations. These properties should make this complex useful for NMR thermometry in a wide range of applications. In addition, the ^{1}H and ^{31}P resonance lines of Tm-DOTP^{5-} are separated by hundreds of parts per million from

those of diamagnetic molecular species, so the NMR signals from the complex do not overlap lines that are native to biological tissue. It may prove practical to use this method to measure temperature and pH distributions *in vivo* with low magnetic field strengths and relatively poor field homogeneities.

ACKNOWLEDGMENTS

REFERENCES

1. E. Cady, P. D'Souza, J. Penrice, and A. Lorek, *Magn. Reson. Med.* **33,** 862–867 (1995).

2. H. Cline, K. Hynynen, C. Hardy, R. Watkins, J. Schenck, and F. Jolesz, *Magn. Reson. Med.* **31,** 628–636 (1994).

3. H. Cline, K. Hynynen, E. Schneider, C. Hardy, S. Maier, R. Watkins, and F. Jolesz, *Magn. Reson. Med.* **35,** 309–315 (1996).

4. J. De Poorter, C. De Wagter, Y. De Deene, C. Thomsen, F. Stahlberg, and E. Achten, *Magn. Reson. Med.* **33,** 74–81 (1995).

5. J. De Poorter, C. De Wagter, Y. De Deene, C. Thomsen, F. Stahlberg, and E. Achten, Proceedings of the Society of Magnetic Resonance in Medicine, 12th Annual Meeting, New York, p. 738, 1993.

6. J. Delannoy, C. Chen, R. Turner, L. Levin, and D. Le Bihan, *Magn. Reson. Med.* **19,** 333–339 (1991).

7. C. Hardy, H. Cline, and R. Watkins, *J. Comput. Assist. Tomogr.* **18,** 476–483 (1994).

8. D. Le Bihan, J. Delannoy, and R. Levin, *Radiology* **171,** 853–857 (1989).

9. T. Samulski, J. MacFall, Y. Zhang, W. Grant, and C. Charles, *J. Hyperthermia* **8,** 819–829 (1992).

10. C. Schwarzbauer, J. Zange, H. Adolf, R. Deichmann, U. Noth, and A. Haase, *J. Magn. Reson. B* **106,** 178–180 (1995).

11. H. Shukla, R. Mason, D. Woessner, and P. Antich, *J. Magn. Reson. B* **106,** 131–141 (1995).

12. I. Young, J. Hand, A. Oatridge, M. Prior, and G. Forse, *Magn. Reson. Med.* **31,** 342–345 (1994).

13. J. De Poorter, C. De Wagter, Y. De Deene, C. Thomsen, F. Stahlberg, and E. Achten, *J. Magn. Reson. B* **103,** 234–241 (1994).

14. B. Berkowitz, J. Handa, and C. Wilson, *NMR in Biomedicine* **5,** 65–68 (1992).

15. A. Abragam, ''Principles of Nuclear Magnetism,'' Oxford Univ. Press, Oxford (1961).

16. B. Bernheim, H. Gutowsky, and D. Woessner, *J. Chem. Phys.* **30,** 950–956 (1959).

17. B. Bleaney, *J. Magn. Reson.* **8,** 91–100 (1972).

18. N. Bloembergen and L. O. Morgan, *J. Chem. Phys.* **34,** 842–850 (1961).

19. R. Drago, J. Zink, R. Richman, and W. Perry, *J. Chem. Educ.* **51,** 371–376, 464–467 (1974).

20. R. A. Dwek, ''NMR in Biochemistry,'' Clarendon, Oxford (1973).

21. C. S. Zuo, J. L. Bowers, K. R. Metz, T. Nosaka, A. D. Sherry, and M. E. Clouse, *Magn. Reson. Med.* **36,** 955–959 (1996).

22. T. Frenzel, K. Roth, S. Kobler, B. Raduchel, H. Bauer, J. Platzek, and H.-J. Weinmann, *Magn. Reson. Med.* **35,** 364–369 (1996).

23. S. Aime, M. Botta, M. Fasano, E. Terreno, P. Kinchesh, L. Calabi, and L. Paleari, *Magn. Reson. Med.* **35,** 648–651 (1996).

24. N. Butwell, R. Ramasamy, A. Sherry, and C. Malloy, *Invest. Radiol.* **26,** 1079–1082 (1991).

25. N. Bansal, M. Germann, I. Lazar, C. Malloy, and A. D. Sherry, *J. Magn. Reson. Imag.* **2,** 385–391 (1992).

26. N. Bansal, M. Germann, V. Seshan, G. Shires, C. Malloy, and A. D. Sherry, *Biochemistry* **32,** 5638–5643 (1993).

27. D. Buster, M. Castro, C. Geraldes, C. Malloy, A. D. Sherry, and T. Siemers, *Magn. Reson. Med.* **15,** 25–32 (1990).

28. R. Bates, ''Determination of pH: Theory and Practice,'' Wiley, New York (1973).

29. C. F. G. C. Geraldes, A. D. Sherry, and G. E. Kiefer, *J. Magn. Reson.* **97,** 290–304 (1992).

30. J. Ren and A. D. Sherry, *Inorg. Chim. Acta* **246,** 331–341 (1996).